# Microscale Colocalization of Cascade Enzymes Yields Activity Enhancement

Yan Xiong<sup>1#</sup>, Stanislav Tsitkov<sup>2#</sup>, Henry Hess<sup>2</sup>, Oleg Gang<sup>1,3,4\*</sup>, Yifei Zhang<sup>5,6\*</sup>

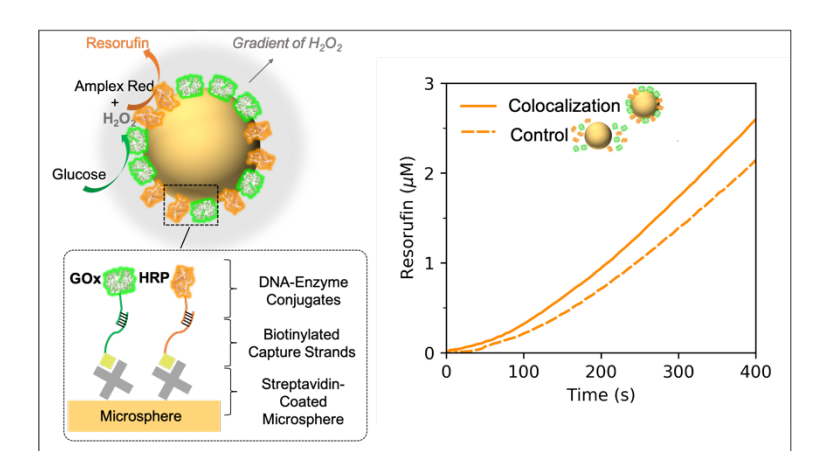
- 1. Department of Chemical Engineering, Columbia University, New York, NY 10027, USA
- 2. Department of Biomedical Engineering, Columbia University, New York, NY 10027, USA
- 3. Department of Applied Physics and Applied Mathematics, Columbia University, New York, NY 10027, USA
- 4. Center for Functional Nanomaterials, Brookhaven National Laboratory, Upton, NY 11973, USA
- 5. State Key Laboratory of Chemical Resource Engineering, Beijing University of Chemical Technology, Beijing 100029, China
- 6. Beijing Advanced Innovation Center for Soft Matter Science and Engineering, Beijing University of Chemical Technology, Beijing 100029, China

<sup>&</sup>lt;sup>#</sup> These authors contributed equally to this work.

<sup>\*</sup> Email address: og2226@columbia.edu; yifeizhang@mail.buct.edu.cn

#### **Abstract**

Colocalization of cascade enzymes is broadly discussed as a phenomenon that can boost the cascade reaction throughput, although a direct experimental verification is often challenging. This is mainly due to difficulties in establishing proper size regimes and in the analytical quantification of colocalization effect with adequate experimental systems and simulations. In this study, by taking advantage of reversible DNA-directed colocalization of enzymes on microspheres, we established a cascade system that can be used to directly evaluate the colocalization effect with exactly the same experimental settings except for the state of enzyme dispersion. In the regime of highly dilute microspheres of particular sizes, the colocalized cascade shows enhanced activity compared with the freely diffusing cascade, as evidenced by a shortened lag phase in the time-course production. Reaction-diffusion modeling reveals that the enhancement can be ascribed to the initial accumulation of intermediate substrate around the colocalized enzymes and is found to be carrier size-dependent. This work demonstrates the dependence of the colocalization effect of enzyme cascades on an interplay of nano- and microscales, lending theoretical supports to the rational design of high-efficient multienzyme catalysts.



For Table of Contents Only

# **Keywords**

colocalization, enzyme cascade, activity enhancement, DNA strand-displacement reaction, substrate channeling

## Introduction

Implementing multistep chemical synthesis by enzyme cascades has begun to reshape industrial chemical production, <sup>1,2</sup> pharmaceutical manufacturing, <sup>3</sup> and environmental remediation. <sup>4</sup> A recent landmark achievement was the development of a nine-enzyme, three-step enzymatic approach for the synthesis of islatravir, an investigational HIV drug. <sup>3</sup> Cascade enzymatic catalysis enables sequential reactions to occur in one pot with high activity and extraordinary stereoselectivity without requiring the isolation of intermediates, showing advantages over conventional chemical synthesis. Inspired by biological enzyme cascade reactions which frequently feature co-localization of enzymes on scaffolds, designed cascade enzyme systems have been constructed with elaborate nano-/micro-scale architectures, <sup>5</sup> advancing a broad range of applications in catalysis and biochemical biosensors. <sup>12-14</sup> Interestingly, the controlled placement of enzymes frequently yielded enhanced activity compared to their freely diffusing counterparts, <sup>7,9-18</sup> and the ability to engineer artificial scaffolds holds a great potential for manipulating cascade reactions. <sup>17</sup>

The activity enhancement was initially ascribed to the facilitated transport of intermediate substrates between colocalized enzymes, <sup>7,20-23</sup> resembling a substrate channeling effect that often occurs in multidomain enzymes or multienzyme complexes. <sup>24</sup> However, our previous theoretical analysis has pointed out that facilitating transport only accelerates throughput when the transport of intermediates is a limiting factor, which is the case if the enzymes are separated by micrometer and millimeter distances but not by nanometer distances. <sup>25</sup> We then experimentally demonstrated that a nanometer separation between glucose oxidase (GOx) and horseradish peroxidase (HRP) obtained by directly conjugating the enzymes together does not result in activity enhancement, <sup>26</sup> and that the observed enhancement can originate from the microenvironmental effects of scaffolds on the enzyme activity. <sup>27,28</sup> These insights have been recently echoed by the failure to find substrate channeling in the AROM complex, a compact and multifunctional assembly of ten enzymatic domains that belongs to the shikimate metabolic pathway. <sup>29</sup> Natural substrate channeling at the nanoscale often succeeds because it relies on physical tunnels, as promoted by local effects

associated with charges, pH, molecular arrangements etc., or interfaces to constrain and transfer substrates rather than enzyme colocalization.<sup>30-32</sup> The previous observations of enhancements in coupled activity of enzymes colocalized on nanoscale scaffolds may have intricate origins,<sup>33-36</sup> as at the nanoscale the diffusion of small molecules should not be a rate-limiting step in most enzyme cascades.<sup>25</sup>

If the nanoscale proximity between cascade enzyme pairs cannot directly lead to substrate channeling, can the microscale colocalization make a difference? Here we expand our experimental study from the molecular scale to the micrometer scale and compare the throughput of the GOx-HRP cascade when the enzymes are freely diffusing and when they are immobilized on microspheres of varying sizes. In this cascade, often used as a model system, GOx first oxidizes glucose and produces hydrogen peroxide which further reacts with HRP. The comparison is greatly facilitated by employing reversible DNA hybridization to control enzyme attachments onto microspheres. Since the enzymes can be released from the microspheres by the addition of displacing DNA strands, the cascade throughput of immobilized and free enzymes can be compared for the exact same batch of enzymes, greatly reducing potential artifacts. A shortened lag phase in the production curve is observed for the GOx-HRP cascade colocalized on the surface of microspheres compared with the control with enzymes released, indicating an apparent temporary enhancement in reaction throughput due to channeling. Reaction-diffusion modeling reveals that this enhancement originates from the rapidly established relatively higher intermediate concentration of hydrogen peroxide at the surface of the microspheres, enabling the second enzyme, HRP, to more rapidly convert the hydrogen peroxide intermediate. A new factor entering the description of the reaction-diffusion system is that the sedimentation of larger microspheres, which also affects the cascade activity. This work provides a quantitative understanding of the colocalization effect of cascade enzymes, which is essential for rational design of high-efficient multienzyme catalysts.

# **Results and Discussion**

**DNA-directed colocalization of GOx and HRP.** The colocalization of GOx and HRP was achieved by DNA-directed immobilization<sup>33,34,37</sup> onto streptavidin-coated microspheres, where a

hybridization of DNA strands with attached GOx and HRP respectively allows for placement of enzymes on the microsphere surface through the biotin-streptavidin interaction (referred to as "CO", Figure 1a). As 5.65 µm diameter microspheres are 1000 times larger in size than enzyme molecules, the immobilized enzymes form a two-dimensional single layer on the surface of a microsphere. Given a random distribution of two types of single stranded DNA (DNA1\* and DNA2\*) on a microsphere surface, it is expected that GOx and HRP are distributed randomly in a thin layer on the microsphere. We first functionalized GOx and HRP with maleimide groups and then conjugated them respectively with single-stranded DNA1 and DNA2 through the thiol–maleimide "click" reaction. Each of the DNA strands possesses a 15-base sticky end at the 3' end (Supporting Information Section 1.1, Figure S3). The average molecular ratio of DNA1 to GOx in the purified conjugates is 1.2, and that of DNA2 to HRP is 1.7. Their complementary capture strands DNA1\* and DNA2\*, bearing biotin moieties at their 5' ends, serve as linkers between the streptavidin-coated microspheres and DNA-enzyme conjugates.

The colocalization of GOx and HRP was accomplished through four steps (Figure 1b, Supporting Information Section 1.4): (1) functionalizing the surface of microspheres with equimolar amounts of capture strands DNA1\* and DNA2\*; (2) differential centrifugation to remove excessive capture strands; (3) successive incubation of equimolar DNA1-GOx and DNA2-HRP conjugates with microspheres at room temperature; (4) differential centrifugation to remove excessive unbound DNA-enzyme conjugates. The enzyme immobilization efficacy (bound enzymes/biotin-binding capacity) was determined based on the relative activities of the supernatant prior and post immobilization (Supporting Information Section 1.6 and Figure S6) and was found to be 70% for GOx (corresponding to a surface density of  $4 \times 10^3$  GOx molecules per  $\mu$ m²) and 30% for HRP (corresponding to a surface density of  $2 \times 10^3$  HRP molecules per  $\mu$ m²). The lower efficacy of HRP binding may be attributed to the steric effect caused by the first immobilized GOx, which hinders the access of HRP to its corresponding anchoring sites of DNA2\*.

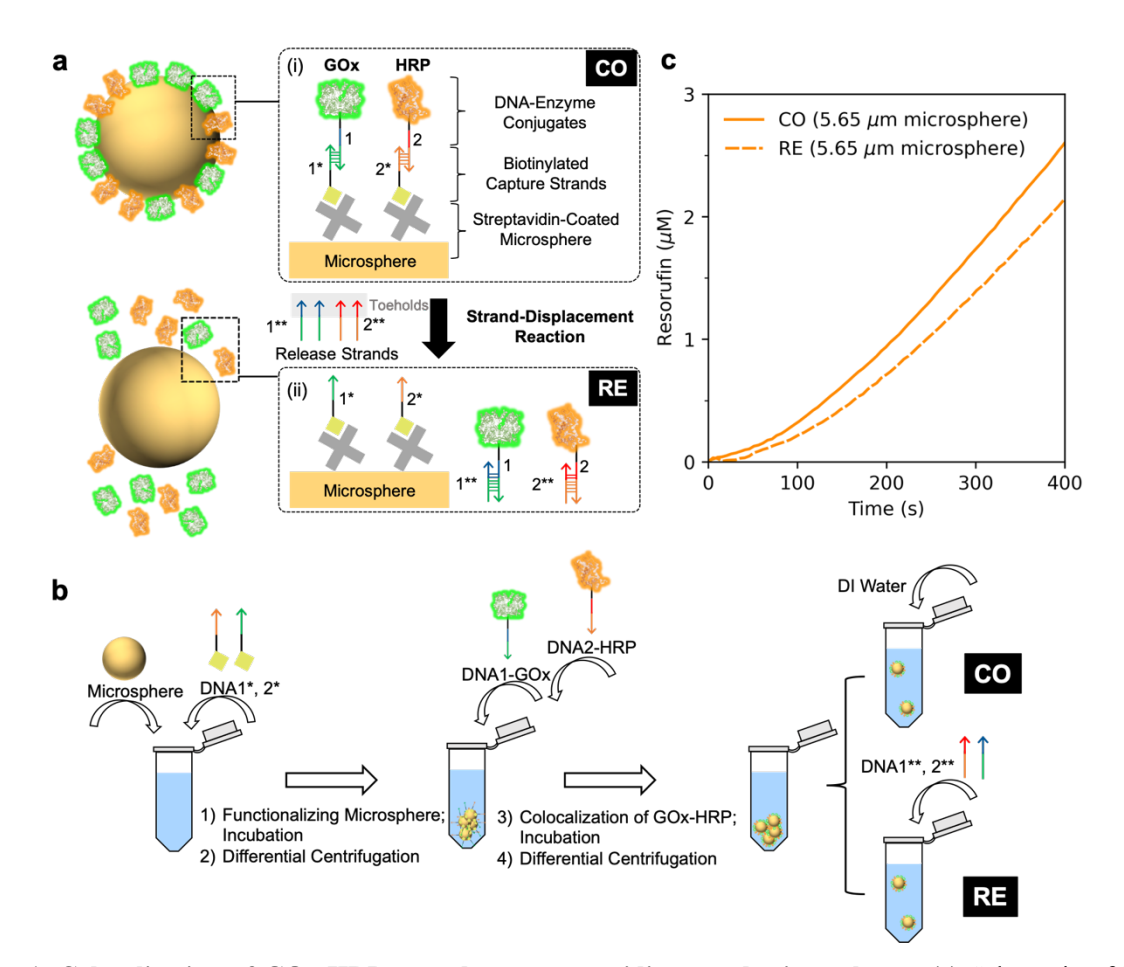


Figure 1. Colocalization of GOx-HRP cascade on streptavidin-coated microspheres. (a) Schematic of DNA-mediated colocalization of GOx and HRP and dissociation through strand-displacement reactions. The biotinylated capture strands bridge microsphere surface (*via* the biotin-streptavidin interaction) and DNA-enzyme conjugates (*via* the DNA hybridization between DNA1 to DNA1\* and DNA2 to DNA2\*, respectively). (i, CO). These DNA-conjugated enzymes are released into the solution upon the addition of release strands *via* toehold-mediated strand-displacement reactions (ii, RE). (b) Illustration of the preparation of the colocalized GOx-HRP sample, CO, and the released control, RE. (c) The time-course production of resorufin by the CO and RE samples (microsphere diameter: 5.65 μm).

The colocalized GOx and HRP can be released into the solution again upon the addition of release strands to initiate toehold-mediated DNA strand-displacement reactions (Figure 1a). The displacement occurs at the toehold regions of the release strands (DNA1\*\* and DNA2\*\*) complementary to the unpaired region of the enzyme-conjugated strands, through which DNA-enzyme conjugates are detached from the microspheres. The addition of 20-fold release strands to the enzyme conjugates resulted in a release efficacy (released enzymes/initially bound enzymes) of nearly 100% for GOx and 60% for HRP (Figure S6). In a

typical experiment, we sequentially immobilized the GOx-DNA1 conjugate and HRP-DNA2 conjugate onto microspheres, and then prepared two identical samples from the same batch of colocalized enzymes. The release strands, DNA1\*\* and DNA2\*\*, were added to one of the samples to release the enzymes from the microspheres (Figure 1b). In this way, we ensured exactly the same amounts of GOx and HRP participating in cascade reactions carried out by the colocalized or the freely diffusing enzymes.

Cascade kinetics of colocalized system and free enzymes. The cascade reactions of GOx and HRP were assayed with a chromogenic substrate, Amplex Red, which can be oxidized to a bright pink product, resorufin.<sup>27</sup> We first investigate if DNA conjugation, hybridization, the presence of excess DNA, and enzyme immobilization onto microspheres alter the activity of individual enzymes (Table S3 and Figure S7). We found no statistically significant difference in catalytic parameters (k<sub>cat</sub> and K<sub>M</sub> values for either GOx or HRP) between the immobilized enzyme-DNA conjugates without and with release strands. In other words, releasing GOx or HRP from the microspheres does not change their individual activity.

The time-course production of resorufin is monitored on an ultraviolet–visible spectrophotometer in the presence of 100 mM glucose (Figures 1c and S5). The colocalized system (CO) shows a higher reaction rate than the released system (RE). The characteristic lag phase originating from the gradual increase in the concentration of intermediate substrate H<sub>2</sub>O<sub>2</sub> is found for both cases. The CO system exhibits a shortened transient phase compared with the RE sample, indicating that the colocalization of GOx and HRP in fact accelerates the cascade reaction. As we have proven that neither the activity of GOx nor HRP decreased after release, this acceleration can only be ascribed to the relatively higher concentration of H<sub>2</sub>O<sub>2</sub> in the enzyme layer produced by the assembled GOx molecules and the rapid consumption of H<sub>2</sub>O<sub>2</sub> by the microsphere-assembled HRP molecules. The more rapid establishment of H<sub>2</sub>O<sub>2</sub> concentration around HRP molecules makes this effect resemble substrate channeling.

To further confirm that colocalization causes a channeling-like effect, we conducted a standard competition assay by introducing catalase (CAT) into the two systems (Figure 2a). Free CAT consumes  $H_2O_2$  primarily in the bulk solution and thus reduces the reaction velocity of the GOx-HRP cascade when the enzymes are released. In comparison, only a small amount of CAT is present in the enzyme

colocalization layer for the on-a-microsphere colocalized system, and diverts only a small portion of the locally generated  $H_2O_2$  away from the HRP. In other words, it is expected that the presence of CAT reduces more effectively the production by free enzymes than by the colocalized enzymes. As shown in Figure 2b, the addition of CAT suppresses the production of resorufin by both the CO and RE systems and the suppression becomes stronger with increasing CAT concentration. The CO system, however, exhibits resistance to the presence of CAT (Figure 2c). The instantaneous velocity ratio,  $V_{CO}/V_{RE}$ , is approximate in a range of 1.1 - 1.2 in the absence of CAT, while it is increased to the ranges of 1.2 - 1.3 and 1.3 - 1.7 in the presence of 0.65 nM and 1.3 nM CAT, respectively. This indicates that the colocalization of enzymes "channels"  $H_2O_2$  molecules towards HRP and prevents the diversion of  $H_2O_2$  by CAT.

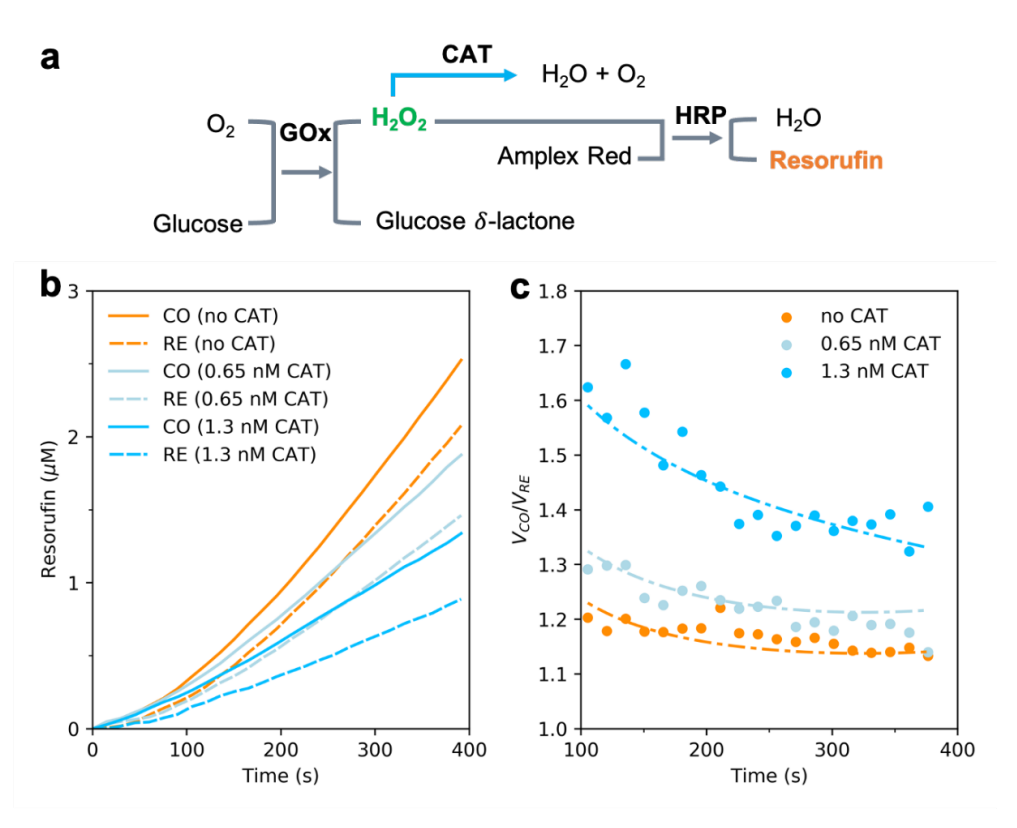
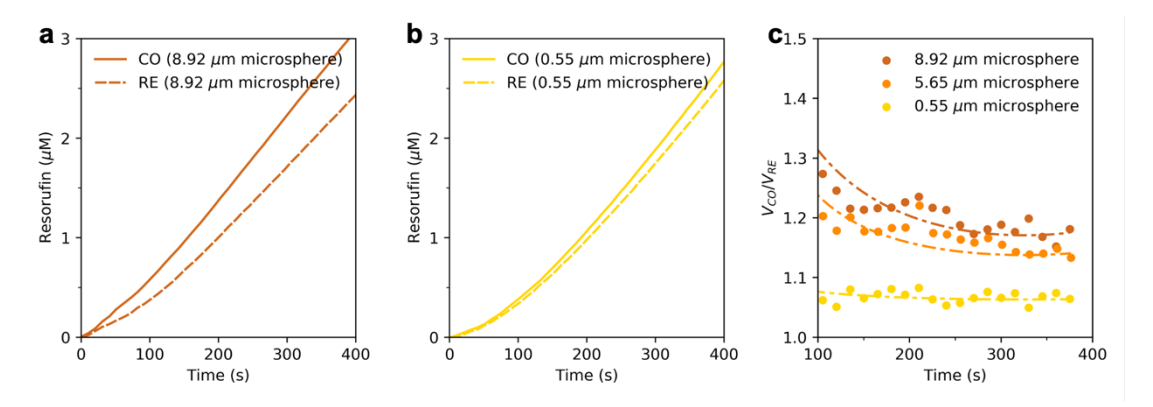


Figure 2. The colocalized (CO) and released (RE) GOx-HRP cascades in the presence of catalase (CAT). (a) Schematic of GOx-HRP cascade reaction coupled with a competitive reaction of H<sub>2</sub>O<sub>2</sub> decomposition catalyzed by catalase. (b) The production of resorufin as a function of time in the presence of varying concentrations of catalase. (c) The ratio of reaction velocities of colocalized GOx-HRP on microspheres to that of the released case in varying concentrations of catalase. Dashed lines represent ratios of smoothed production curves of CO to that of RE in (b).

Support size-dependence of the colocalization effect. We further investigate if the colocalization effect depends on the size of supporting microspheres. We colocalized GOx and HRP onto streptavidin-coated microspheres with varying sizes from 0.55  $\mu$ m to 8.92  $\mu$ m (Figure 3). As the binding capacity of the different microsphere sizes differs, the absolute reaction velocities are not comparable, but the relative velocity between the CO and RE systems from the same batch indicates the effectiveness of the colocalization effect. Figure 3 shows that the 8.92  $\mu$ m microspheres exhibit a more significant colocalization effect than the 0.55  $\mu$ m microspheres, and the enhancement shows a dependence on support size with  $\frac{V_{CO}}{V_{RE}}(8.92 \ \mu m) > \frac{V_{CO}}{V_{RE}}(5.65 \ \mu m) > \frac{V_{CO}}{V_{RE}}(0.55 \ \mu m)$ .



**Figure 3.** The size-dependence of the colocalization effect. The lag phase shortening for GOx-HRP cascade colocalized on (a) 8.92 μm microspheres is more significant than that for the enzymes colocalized on (b) 0.55 μm microspheres. (c) The ratio of reaction velocities of colocalized GOx-HRP on microspheres to that of the released case in varying microsphere size. Dashed lines represent ratios of smoothed production curves of CO to that of RE in (b).

Modeling of colocalized cascade. To gain theoretical insights into cascade colocalization, we construct a reaction-diffusion model for the colocalized cascade and compare its throughput to the free enzymatic reaction. Our model places an individual microsphere of radius R at the center of a spherical container of radius L whose volume is equal to the inverse of the microsphere concentration (Figure 4a). The microsphere is coated with GOx and HRP with given surface densities. The concentrations of substrate (glucose) and intermediate ( $H_2O_2$ ) molecules as a function of the radial distance from the center of the container are modeled using the diffusion equation. The Michaelis-Menten kinetics of the enzymes, GOx

and HRP, are implemented as flux boundary conditions on the surface of the microsphere, while reflecting (zero flux) boundary conditions are implemented at the boundary of the container (Supporting Information Section 2.1).

We first simulated the case of GOx-HRP colocalization in the absence of any competing or interfering reaction, using the enzyme parameters shown in Table S3. The time- and radius-dependent concentration of  $H_2O_2$  molecules is shown in Figure 4b. It is noteworthy that there exists no steady state as the concentration of  $H_2O_2$  increases all the time and so does the reaction throughput. The highest concentration of  $H_2O_2$  always occurs at the microsphere surface (R=0). As the reaction progresses, the  $H_2O_2$  spread into the bulk solution ( $r > 20 \,\mu m$ ) with a significant time lag (400 s). The  $H_2O_2$  concentration at the surface of the microsphere shows the rapid rise indicative of channeling which creates the more rapid production of resorufin compared to the free reaction (Figure 4c). The concentration of  $H_2O_2$  at the surface of the microsphere reaches a quasi-steady state on a time scale (30 ms) that is dependent on the kinetic parameters of HRP and the radius of the microsphere (Supporting information Section 2.2.3). This simulation matches the experimental results in Figure 1c.

In the framework of the channeling effect, the channeling fraction  $f_{channel}$  defined by the initial ratio of resorufin production by HRP and  $H_2O_2$  production by GOx is given by (Supporting Information Section 2.2):

$$f_{channel} = \frac{V_{\text{HRP,inital}}}{V_{\text{GOx,initial}}} = \frac{1}{\left(\frac{DK_{M}N_{A}}{Rk_{cat}\sigma} + 1\right)}$$
(1)

where D is the diffusion coefficient of  $H_2O_2$ ,  $k_{cat}$  is the catalytic rate constant of HRP,  $K_M$  is the Michaelis-Menten constant of HRP,  $\sigma$  is the surface density of HRP,  $N_A$  is Avogadro's number, and R is the radius of the microsphere. The channeling fraction can be interpreted as the probability that an intermediate molecule generated at the surface of the microsphere will be converted into product before diffusing away into the bulk. As expected<sup>25</sup> and consistent with the results shown in Figure 3c, the channeling fraction increases with the radius of the microsphere if the enzyme surface density is constant: the channeling fraction is 0.6% for a 0.55  $\mu$ m microsphere, 6% for a 5.65  $\mu$ m microsphere, and 9% for an

8.92 µm microsphere. This effect is mainly because a larger microsphere provides a larger number of potential active sites for intermediate molecules to react before escaping into the bulk, and thus a higher conversion is expected. Considering that it is just an extremely thin layer of colocalization, the boost in cascade throughput is noticeable although the channeling fraction seems relatively small. For example, the colocalization on 8.92 µm microspheres lead to a 30% increase in productivity within 400 seconds compared to the released case. As the concentration of microspheres (or free enzymes) is extremely dilute, building up a substantial concentration of H<sub>2</sub>O<sub>2</sub> in the bulk solution takes a long time. Colocalization of cascade enzymes reduces the chance for the *in situ* produced H<sub>2</sub>O<sub>2</sub> escaping before being taken by HRP, thus a small fraction of H<sub>2</sub>O<sub>2</sub> directly flux to the local HRP molecules at the very initial stage would lead to a significant contribution to the reaction throughput. It is noteworthy that such colocalization results in "leaky" channeling that a large portion of intermediate substrates still diffuse to the bulk solution. Equation (1) implies that the channeling fraction can be further improved by increasing the surface density of enzymes, or reducing the diffusivity of intermediates (for example, by increasing the viscosity of reaction media).

To simulate the presence of a competing reaction, an additional reaction rate proportional to concentration is added to the diffusion equation of the intermediate describing the kinetics below the  $K_M$  of the competing enzyme (Supporting Information Section 2.4). At steady state and in the linear regime, the resorufin throughput can be solved for in a closed form for the colocalized case (Supporting Information Section 2.4). A comparison of the steady state resorufin throughput for the colocalized and free reactions in the presence of varying concentrations of catalase (with catalytic efficiency of 3  $\mu$ M<sup>-1</sup> s<sup>-1</sup>) is plotted in Figure 4d. It is noteworthy that in the simulation the benefits of colocalization in the presence of a competing enzyme are more pronounced than in the experiments (Figure 2c). This is likely due to a smaller channeling fraction in the experiments arising from a lower than estimated enzyme surface density due to defects in the streptavidin coating and DNA functionalization of the microsphere surface leading to an inhomogeneous distribution of enzymes.<sup>40</sup> The discontinuous coverage of enzymes significantly hinders the local enrichment and conversion of  $H_2O_2$  around the microsphere surface.

Equation 1 indicates that the channeling fraction  $f_{channel}$  increases with increasing microsphere size, albeit with diminishing returns for microsphere radii greater than  $DK_MN_A/k_{cat}\sigma$ . However, Equation 1 does not consider potential transport limitations for the supply of the substrate (glucose) for the first enzyme in the cascade (GOx), which may emerge with increasing microsphere size. The increase in microsphere size while keeping enzyme surface density constant will lead to faster consumption of substrate at the microsphere surface, forming a depletion zone of substrate molecules. In Supporting Information Section 2.5, we show that the depletion zone formed near the microsphere surface is not sufficient to adversely affect the initial reaction throughput in this system. Thus, under the assumptions of the model, increasing the microsphere size will always increase the cascade throughput.

We then attempt to establish an upper bound on microsphere size. A key observation that allows us to define a maximum size of the microsphere is the sedimentation phenomenon, where microspheres would settle down over time due to gravity, resulting in a local enrichment of microspheres and thus the colocalization of enzymes at the bottom of the cuvette (Supporting Information Section 1.8). The sedimentation alters the distribution of substrate, intermediate and product molecules near the microsphere surface due to the fluid flow. A parallel may be drawn between our settling microspheres and the motile single-cellular organisms analyzed by Berg and Purcell. They noted that single-cellular organisms would only avoid depletion zones of molecules forming around them if their speed overcame the rate of diffusive transport of those molecules. Roughly, if v is the velocity of the organism, D is the diffusion coefficient of the molecule, and L is the length of the organism, then the depletion layer does not form if:

$$v > \frac{D}{L} \tag{2}$$

In our study, the goal is the opposite: to maintain the enhanced concentration of  $H_2O_2$  molecules at the surface. Substituting v with the settling velocity of the microsphere, substituting v with the radius of the microsphere, and changing the direction of the equality, we obtain the following expression for the maximum radius to observe enhancement of throughput:

$$\frac{2}{9} \cdot \frac{\left(\rho_{sphere} - \rho_{fluid}\right)gR^2}{\eta} < \frac{D}{R} \tag{3}$$

where  $\rho_{sphere}$  is the density of the microsphere with values on the range of 1.3-2.3 g cm<sup>-3</sup>,  $\rho_{fluid}$  is the density of the fluid (1 g cm<sup>-3</sup>), g is the acceleration of gravity,  $\eta$  is the viscosity, and D and R are defined as before. The radius of the microsphere thus has to be smaller than  $10-30~\mu m$ , or the fluid flow arising from rapid sedimentation will wash away the enhanced concentration of  $H_2O_2$  molecules at the surface of the microsphere. While the microspheres used by us are smaller, they already exhibit sedimentation on the timescale of the experiments but not on the timescale of the initial lag phase (Figure S8). To avoid sedimentation of larger microspheres, in practice, stirring the reaction system is often required, but the stirring-induced flow would further reduce the channeling-like effect. Besides sedimentation, recent studies have indicated that surface-immobilized enzymes can pump the surrounding fluid through reaction-induced flow.<sup>42,43</sup> It is possible that the fluid flow could speed up enzymatic reactions by increasing substrate fluxes. However, given the glucose concentration in our system is saturated for glucose oxidase, the fluid flow around the microsphere is more likely to reduce the cascade activity by interfering the local enrichment of  $H_2O_2$ . Also, as our modeling without considering any flows fits well the experimental results, the reaction-induced flow is unlikely to play a significant role in our system.

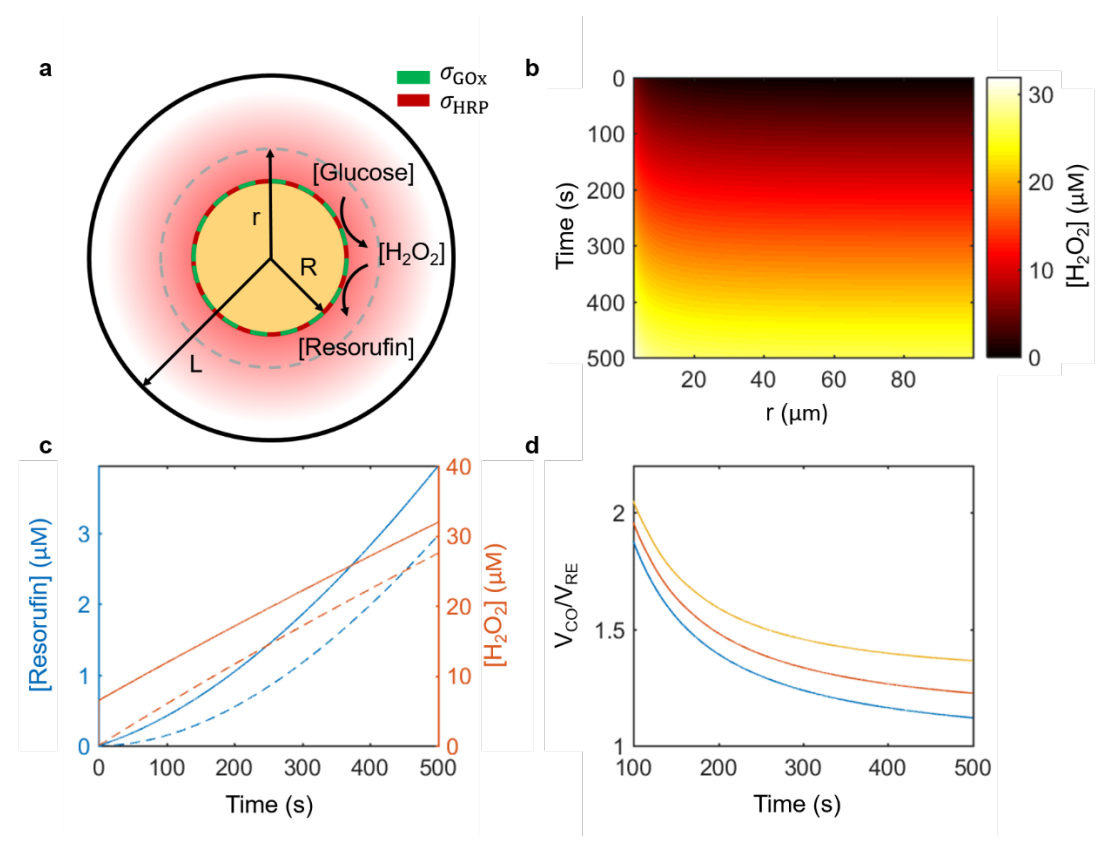


Figure 4. Reaction diffusion modeling of colocalized cascade reaction. (a) Diagram of the reaction diffusion model for the colocalized cascade. (b) Heatmap of H<sub>2</sub>O<sub>2</sub> concentration as a function of radius from the center of the microsphere and time. (c) Left axis (blue): Total resorufin produced as a function of time in the colocalized cascade (solid line) and free reaction (dashed line). Right axis (red): Concentration of H<sub>2</sub>O<sub>2</sub> as a function of time at the surface of the microsphere in the colocalized reaction (solid line) and in the bulk solution in the free reaction (dashed line). (d) Velocity of colocalized reaction over velocity of free reaction as a function of time in the presence of catalase at concentrations of 0 nM (purple line), 0.65 nM (red line), 1.3 nM (orange line).

## **Conclusions**

The concept that colocalization of cascade enzymes can enhance reaction activity is intuitive and widely accepted, but in practice, colocalization does not always result in activity enhancement due to inevitable factors such as deactivation of enzymes and mass transfer resistance caused by immobilization. On the other hand, the appearance of activity enhancement after enzyme colocalization is insufficient evidence for a colocalization effect if the effect of the scaffold on the enzyme is not accounted for. In this work, we demonstrate a strategy for directly evaluating the colocalization effect by reversible colocalization of cascade enzymes on microspheres of varying sizes, and uncover in which size regime the colocalization

affects the cascade throughput. The thin-layer colocalization of enzymes on microspheres minimizes the potential resistance to diffusion and the reversible DNA hybridization offers access to an adequate delocalized control. We confirm the colocalization-induced activity enhancement based on the shortened characteristic lag phase in the production curve together with a standard catalase competition experiment. Reaction-diffusion modeling reveals that the colocalization effect is a consequence of the rapid establishment of a relatively high concentration of H<sub>2</sub>O<sub>2</sub> at the microsphere surface where the cascade reactions are therefore accelerated. This effect resembles the classic substrate channeling and is found to be support size-dependent, which can be quantitatively evaluated by a channeling fraction. The reaction-diffusion model considers Michaelis-Menten kinetics of enzymes and the diffusion of reactants; and it should be applied to other colocalized multienzyme systems. Given that H<sub>2</sub>O<sub>2</sub> is almost the smallest intermediate substrate, other systems with larger intermediate substrates could have more kinetic benefits from microscale colocalization. For the enzyme cascades involving the regeneration of coenzymes, although in principle this channeling-like effect exists, these cascades are often significantly affected by the reaction equilibrium and substrate/product inhibition.<sup>28</sup> Thus, the kinetic behaviors of these systems may be more complicated than the prediction by our model.

Colocalization of cascade enzymes is also a strategy taken by living cells to regulate metabolic fluxes through the formation of temporary enzyme-enzyme assemblies, often referred to as metabolons.<sup>44-47</sup> It is believed that metabolons can mediate substrate channeling, and the proof is mainly relying on the identification of protein-protein interactions and kinetic analysis.<sup>48</sup> Interestingly, many metabolons are found to be associated with structural elements such as the cytoskeleton and various membranes.<sup>44,37-51</sup> Our work demonstrates again that mere colocalization of cascade enzymes at the nanoscale scale may be ineffective in channeling intermediate substrates under the assumption that intermediates undergo free diffusion. Therefore, other factors such as specific interactions between substrates and protein domains and allosteric effects may play more vital roles in the activity regulation and need to be accounted for. Cascade enzymes have also been engineered to display on the surface of microbial cells such as yeasts *Saccharomyces cerevisiae* and *Kluyveromyces marxianus* and increments in production by multienzyme

systems were frequently reported.<sup>52-55</sup> As the size of typical microbial cells is similar to the microspheres employed in this study, our findings lend solid support to the cell-surface display technique for anchoring cascade enzymes.

#### Methods

**Materials.** GOx from *Aspergillus niger* (type VII), HRP, <sub>D</sub>-glucose, H<sub>2</sub>O<sub>2</sub> (30 wt.% in water), tris(2-carboxyethyl)phosphine (TCEP) and Amplex red were purchased from Sigma Aldrich Co. LLC. Succinimidyl-4-(N-maleimidomethyl)cyclohexane-1-carboxy-(6-amidocaproate) (LCSMCC) was purchased from ThermoFisher Scientific, Inc., USA. Oligonucleotides were purchased from Integrated DNA Technologies, Inc., USA. Microspheres were purchased from Spherotech Inc., USA.

Synthesis of DNA-enzyme conjugate. Enzymes were first mixed with LC-SMCC at a ratio of 1:100 in PBS (pH=7.4) and incubated for 30 min at room temperature, and then purified by passing through a HiTrap desalting column (prepacked with G-25, 5 mL). Thiolated oligonucleotides were first reduced by TCEP at a ratio of 1:1000 in DI water, followed by the removal of excess of TCEP with a size-exclusion column (G-25, GE Healthcare). The SMCC-modified enzymes were then mixed with the activated oligonucleotides at a ratio of 1:3 in PBS buffer (pH 7.4) and incubated at room temperature for 2 h. The obtained DNA-enzyme conjugates were purified by ultracentrifugation with Amicon® Ultra Centrifugal Filters with a molecular weight cut-off (MWCO) of 50 kDa.

Colocalization of cascade enzymes. Streptavidin-coated microspheres were first mixed with biotinylated capture strands (the amount of the capture stands is 2-fold of biotin-based binding capacity of microspheres), followed by overnight incubation at room temperature. Differential centrifugation was carried out to remove unbound strands. Next, the DNA-enzyme conjugates were introduced stepwise into the purified microsphere suspension (ratio of DNA strand of conjugate to biotin-based capacity of microsphere is 2:1). After 7 h incubation at room temperature, the mixture was subject to differential centrifugation to remove unbound enzymes.

Enzymatic Assay. Enzyme quantifications were carried out on an ultraviolet-visible spectrophotometer (Cary 300, Agilent Technologies). Enzymatic activities were measured by monitoring the changes in absorbance at 415 nm by the spectrophotometer (extinction coefficient of ABTS radical cation:  $3.6 \times 10^4 M^{-1} cm^{-1}$ ).

**Reaction-diffusion modeling for colocalized cascade reactions.** The diffusion equations for the colocalized reaction on a microsphere of radius R can be written down as:

$$\frac{d[S]}{dt} = D_S \nabla^2[S] = \frac{D_S}{r^2} \cdot \frac{\partial}{\partial r} \left( r^2 \frac{\partial[S]}{\partial r} \right) \tag{4}$$

$$\frac{d[I]}{dt} = D_I \nabla^2 [I] - k_e[I] = \frac{D_I}{r^2} \cdot \frac{\partial}{\partial r} \left( r^2 \frac{\partial [I]}{\partial r} \right) - k_e[I]$$
 (5)

where [S] and [I] denote concentrations of substrate and intermediate molecules,  $D_S$  and  $D_I$  are diffusion coefficients, r is the distance from the center of the microsphere, and  $k_e$  is the turnover rate of the competing reaction. The reaction on the microsphere surface is treated as a flux boundary condition at r=R:

$$N_A D_S \frac{d[S]}{dr}\bigg|_{r=R} = \frac{k_{cat,1} \sigma_{E1}[S](r=R)}{K_{M,1} + [S](r=R)}$$
(6)

$$N_A D_I \frac{d[I]}{dr}\bigg|_{r=R} = -\frac{k_{cat,1} \sigma_{E1}[S](r=R)}{K_{M,1} + [S](r=R)} + \frac{k_{cat,2} \sigma_{E2}[I](r=R)}{K_{M,2} + [I](r=R)}$$
(7)

where the  $k_{cat,I}$  denotes the catalytic rate constants of the enzymes, the  $K_{M,i}$  denotes the Michaelis-Menten constants of the enzymes, and  $\sigma_i$  denotes the surface densities of the enzymes. The edges of the container are set as reflective boundary conditions:

$$\left. \frac{\partial [S]}{\partial r} \right|_{r=L} = 0 \tag{8}$$

$$\left. \frac{\partial [I]}{\partial r} \right|_{r=L} = 0 \tag{9}$$

The initial concentration of substrate is set to 100 mM and the initial concentration of intermediate is set to 0 mM. The parameter 'L' is chosen such that the total enzymes per available volume of the container is conserved between the colocalized and free reaction.

**Free Reaction Modeling.** The free reactions were modeled using the following set of ordinary differential equations:

$$\frac{d[S]}{dt} = -\frac{k_{cat,1}[E_1][S]}{K_{M,1} + [S]} \tag{10}$$

$$\frac{d[I]}{dt} = \frac{k_{cat,1}[E_1][S]}{K_{M,1} + [S]} - \frac{k_{cat,2}[E_2][I]}{K_{M,2} + [I]} - k_e[I]$$
(11)

$$\frac{d[P]}{dt} = \frac{k_{cat,2}[E_2][I]}{K_{M,2} + [I]} \tag{12}$$

Where all variables are defined as before, [P] denotes the concentration of product molecules, and [E<sub>1</sub>] and [E<sub>2</sub>] denote the concentrations of GOx and HRP, respectively, which are set to 190 pM and 80 pM, respectively. Initial conditions are set to:  $[S_0] = 100$  mM, and  $[I_0] = [P_0] = 0$  mM. In order to preserve consistency between the colocalized and free reaction, the container outer radius (L) is chosen such that the number of enzymes divided by the available volume for diffusion is the equal to the concentration of the enzyme in the free reaction:

$$[E_i] = \frac{n_{Ei}}{\frac{4}{3}\pi L^3 - \frac{4}{3}\pi R^3} = \frac{4\pi R^2 \sigma_{Ei}}{\frac{4}{3}\pi L^3 - \frac{4}{3}\pi R^3}$$
(13)

The surface density of HRP,  $\sigma_{E1}$ , is set to 2000  $\mu m^{-2}$ . The surface density of GOx,  $\sigma_{E1}$ , is set to maintain the ratio of concentrations of GOx to HRP in the free reaction.

## **Associated Content**

## **Supporting Information**

The Supporting Information is available free of charge on the ACS Publications website at DOI: xxx. Supplementary materials, characterization of DNA-enzyme conjugates, DNA-mediated enzyme immobilization and strand displacement reaction, colocalization of cascade enzymes on microspheres, enzymatic assay, evaluation of co-immobilization and release efficiencies, Michaelis-Menten kinetics of glucose oxidase and horseradish peroxidase, effect of microsphere sedimentation, and modeling (PDF)

# **Acknowledgements**

Y.Z. acknowledges support by the National Key Research & Development Program of China under Grant No. 2021YFC2104100, and the National Natural Science Foundation of China under Grant No. NSFC-22178018. H.H. acknowledges support from the National Science Foundation of the USA under Award Number NSF-ENG 1844149. Y.X and O.G. acknowledge support from the National Science Foundation of USA under Grant No. 1905920.

## **Author information**

#### **Affiliations**

State Key Laboratory of Chemical Resources Engineering, Beijing University of Chemical Technology, Beijing 100029, China

Yifei Zhang

Beijing Advanced Innovation Center for Soft Matter Science and Engineering, Beijing University of Chemical Technology, Beijing 100029, China

Yifei Zhang

Department of Chemical Engineering, Columbia University, New York, NY 10027, USA

Yan Xiong & Oleg Gang

Department of Biomedical Engineering, Columbia University, New York, NY 10027, USA

Stanislav Tsitkov & Henry Hess

Department of Applied Physics and Applied Mathematics, Columbia University, New York, NY 10027,

**USA** 

Oleg Gang

Center for Functional Nanomaterials, Brookhaven National Laboratory, Upton, NY 11973, USA

Oleg Gang

The authors declare no competing interests.

#### **Author contributions**

Y.Z., H.H. and O.G. conceived the concept of this work. Y.X. and Y.Z. designed the research. Y.X. and

Y.Z. performed the experiments. S.T. performed the modeling. All the authors discussed the results. Y.X.,

S.T. and Y.Z. wrote the manuscript with input from all authors.

Y.X. and S.T. contributed equally to this work.

# Reference

- Mutti, F. G., Knaus, T., Scrutton, N. S., Breuer, M. & Turner, N. J. Conversion of alcohols to enantiopure amines through dual-enzyme hydrogen-borrowing cascades. *Science* **349**, 1525-1529 (2015).
- 2 Sarak, S. *et al.* An integrated cofactor/co-product recycling cascade for the biosynthesis of Nylon monomers from cycloalkylamines. *Angew. Chem. Int. Ed.* **60**, 3481-3486 (2021).
- Huffman, M. A. *et al.* Design of an in vitro biocatalytic cascade for the manufacture of islatravir. *Science* **366**, 1255-1259 (2019).
- 4 Knott, B. C. *et al.* Characterization and engineering of a two-enzyme system for plastics depolymerization. *Proc. Natl Acad. Sci. USA* **117**, 25476-25485 (2020).
- Delebecque, C. J., Lindner, A. B., Silver, P. A. & Aldaye, F. A. Organization of intracellular reactions with rationally designed RNA assemblies. *Science* **333**, 470-474 (2011).

- Zhang, G., Quin, M. B. & Schmidt-Dannert, C. Self-assembling protein scaffold system for easy in vitro coimmobilization of biocatalytic cascade enzymes. *ACS Catal.* **8**, 5611-5620 (2018).
- Fu, J., Liu, M., Liu, Y., Woodbury, N. W. & Yan, H. Interenzyme substrate diffusion for an enzyme cascade organized on spatially addressable DNA nanostructures. *J. Am. Chem. Soc.* **134**, 5516-5519 (2012).
- 8 Xiong, Y., Huang, J., Wang, S.-T., Zafar, S. & Gang, O. Local environment affects the activity of enzymes on a 3D molecular scaffold. *ACS Nano* **14**, 14646-14654 (2020).
- 9 Vranish, J. N. *et al.* Enhancing coupled enzymatic activity by colocalization on nanoparticle surfaces: kinetic evidence for directed channeling of intermediates. *ACS Nano* **12**, 7911-7926 (2018).
- Linko, V. et al. DNA-Based Enzyme Reactors and Systems. Nanomaterials 6, 139 (2016).
- Davis, B. W. *et al.* Colocalization and sequential enzyme activity in aqueous biphasic systems: experiments and modeling. *Biophys. J.* **109**, 2182-2194 (2015).
- Shi, J.; Wu, Y.; Zhang, S.; Tian, Y.; Yang, D.; Jiang, Z., Bioinspired construction of multi-enzyme catalytic systems. *Chem. Soc. Rev.* **2018**, *47* (12), 4295-4313.
- Bugada, L. F.; Smith, M. R.; Wen, F., Engineering spatially organized multienzyme assemblies for complex chemical transformation. *ACS Catal.* **2018**, *8* (9), 7898-7906.
- Vázquez-González, M.; Wang, C.; Willner, I., Biocatalytic cascades operating on macromolecular scaffolds and in confined environments. *Nat. Catal.* **2020**, *3* (3), 256-273.
- Wilner, O. I. *et al.* Enzyme cascades activated on topologically programmed DNA scaffolds. *Nat. Nanotechnol.* **4**, 249-254 (2009).
- You, C., Myung, S. & Zhang, Y.-H. P. Facilitated substrate channeling in a self-assembled trifunctional enzyme complex. *Angew. Chem. Int. Ed.* **51**, 8787-8790 (2012).
- Jia, F., Narasimhan, B. & Mallapragada, S. K. Biomimetic multienzyme complexes based on nanoscale platforms. *AIChE J.* **59**, 355-360 (2013).
- Rocha-Martín, J., Rivas, B. d. l., Muñoz, R., Guisán, J. M. & López-Gallego, F. Rational co-immobilization of bi-enzyme cascades on porous supports and their applications in bio-redox reactions with in situ recycling of soluble cofactors. *ChemCatChem* **4**, 1279-1288 (2012).
- Ellis, G. A. *et al.* Artificial multienzyme scaffolds: pursuing in vitro substrate channeling with an overview of current progress. *ACS Catal.* **9**, 10812-10869 (2019).
- Zhang, Y. H. P. Substrate channeling and enzyme complexes for biotechnological applications. *Biotechnol. Adv.* **29**, 715-725 (2011).
- Bauler, P., Huber, G., Leyh, T. & McCammon, J. A. Channeling by proximity: the catalytic advantages of active site colocalization using brownian dynamics. *J. Phys. Chem. Lett.* **1**, 1332-1335 (2010).
- Cao, Y. *et al.* Investigating the origin of high efficiency in confined multienzyme catalysis. *Nanoscale 11*, 22108-22117 (2019).
- Shi, J. *et al.* Bioinspired construction of multi-enzyme catalytic systems. *Chem. Soc. Rev.* 47, 4295-4313 (2018).
- Wheeldon, I. et al. Substrate channelling as an approach to cascade reactions. Nat. Chem. 8, 299-309 (2016).

- Idan, O. & Hess, H. Origins of activity enhancement in enzyme cascades on scaffolds. *ACS Nano* 7, 8658-8665 (2013).
- Zhang, Y., Tsitkov, S. & Hess, H. Proximity does not contribute to activity enhancement in the glucose oxidase-horseradish peroxidase cascade. *Nat. Commun.* 7, 13982 (2016).
- Zhang, Y., Wang, Q. & Hess, H. Increasing enzyme cascade throughput by pH-engineering the microenvironment of individual enzymes. *ACS Catal.* 7, 2047-2051 (2017).
- Zhang, Y. & Hess, H. Toward rational design of high-efficiency enzyme cascades. *ACS Catal.* **7**, 6018-6027 (2017).
- Arora Veraszto, H. *et al.* Architecture and functional dynamics of the pentafunctional AROM complex. *Nat. Chem. Biol.* **16**, 973-978 (2020).
- Rhee, S., Parris, K. D., Ahmed, S. A., Miles, E. W. & Davies, D. R. Exchange of K+ or Cs+ for Na+ induces local and long-range changes in the three-dimensional structure of the tryptophan synthase α2β2 complex. *Biochemistry* **35**, 4211-4221 (1996).
- Sanyal, N., Arentson, B. W., Luo, M., Tanner, J. J. & Becker, D. F. First evidence for substrate channeling between proline catabolic enzymes: a validation of domain fusion analysis for predicting protein-protein interactions. *J. Biol. Chem.* **290**, 2225-2234 (2015).
- Tian, Y. *et al.* Ordered three-dimensional nanomaterials using DNA-prescribed and valence-controlled material voxels. *Nat. Mater.* **19**, 789-796 (2020).
- Meyer, R., Giselbrecht, S., Rapp, B. E., Hirtz, M. & Niemeyer, C. M. Advances in DNA-directed immobilization. *Curr. Opin. Chem. Biol.* **18**, 8-15 (2014).
- Sacca, B. & Niemeyer, C. M. Functionalization of DNA nanostructures with proteins. *Chem. Soc. Rev.* **40**, 5910-5921 (2011).
- Vranish, J. N. *et al.* Enhancing coupled enzymatic activity by colocalization on nanoparticle surfaces: kinetic evidence for directed channeling of intermediates. *ACS Nano* **12**, 7911-7926 (2018).
- 36 Chen, W.-H., *et al.* Biocatalytic cascades driven by enzymes encapsulated in metal–organic framework nanoparticles. *Nat. Catal.* **1**, 689-695 (2018).
- Niemeyer, C. M. Self-assembled nanostructures based on DNA: towards the development of nanobiotechnology. *Curr. Opin. Chem. Biol.* **4**, 609-618 (2000).
- Zhang, D. Y. & Seelig, G. Dynamic DNA nanotechnology using strand-displacement reactions. *Nat. Chem.*3, 103-113 (2011).
- 39 Simmel, F. C., Yurke, B. & Singh, H. R. Principles and applications of nucleic acid strand displacement reactions. *Chem. Rev.* **119**, 6326-6369 (2019).
- Arqué, X. et al. Intrinsic enzymatic properties modulate the self-propulsion of micromotors. Nat. Commun.
   10, 2826 (2019).
- 41 Berg, H. C. & Purcell, E. M. Physics of chemoreception. *Biophys. J.* **20**, 193-219 (1977).
- Sengupta, S.; Patra, D.; Ortiz-Rivera, I.; Agrawal, A.; Shklyaev, S.; Dey, K. K.; Cordova-Figueroa, U.; Mallouk, T. E.; Sen, A., Self-powered enzyme micropumps. *Nat. Chem.* **2014**, *6* (5), 415-22.

- Laskar, A.; Shklyaev, O. E.; Balazs, A. C., Self-Morphing, Chemically Driven Gears and Machines. *Matter* **2021**, *4* (2), 600-617.
- French, J. B. *et al.* Spatial colocalization and functional link of purinosomes with mitochondria. *Science* **351**, 733-737 (2016).
- Giege, P. *et al.* Enzymes of glycolysis are functionally associated with the mitochondrion in Arabidopsis cells. *Plant Cell* **15**, 2140-2151 (2003).
- Gou, M., Ran, X., Martin, D. W. & Liu, C. J. The scaffold proteins of lignin biosynthetic cytochrome P450 enzymes. *Nat. Plants* **4**, 299-310 (2018).
- 47 Srere, P. A. The metabolon. *Trends Biochem. Sci.* **10**, 109-110 (1985).
- Zhang, Y. & Fernie, A. R. Metabolons, enzyme-enzyme assemblies that mediate substrate channeling, and their roles in plant metabolism. *Plant Commun.* **2**, 100081 (2021).
- Zhang, Y. *et al.* A moonlighting role for enzymes of glycolysis in the co-localization of mitochondria and chloroplasts. *Nat. Commun.* **11**, 4509 (2020).
- Chan, C. Y., Pedley, A. M., Kim, D., Xia, C. & Zhuang, X. Microtubule-directed transport of purine metabolons drives their cytosolic transit to mitochondria. *Proc. Natl Acad. Sci. USA* **115** (2018).
- Laursen, T. *et al.* Characterization of a dynamic metabolon producing the defense compound dhurrin in sorghum. *Science* **354**, 890-893 (2016).
- Fan, L. H., Zhang, Z. J., Yu, X. Y., Xue, Y. X. & Tan, T. W. Self-surface assembly of cellulosomes with two miniscaffoldins on Saccharomyces cerevisiae for cellulosic ethanol production. *Proc. Natl Acad. Sci. USA* **109**, 13260-13265 (2012).
- Shao, Z. *et al.* Refactoring the silent spectinabilin gene cluster using a plug-and-play scaffold. *ACS Synth. Biol.* **2**, 662-669 (2013).
- Liu, F., Banta, S. & Chen, W. Functional assembly of a multi-enzyme methanol oxidation cascade on a surface-displayed trifunctional scaffold for enhanced NADH production. *Chem. Commun. (Camb)* **49**, 3766-3768 (2013).
- Anandharaj, M. *et al.* Constructing a yeast to express the largest cellulosome complex on the cell surface. *Proc. Natl Acad. Sci. USA* **117**, 2385-2394 (2020).